ANL/NE-16/29

Initial Comparison of Direct and Legacy Modeling Approaches for Radial Core Expansion Analysis

Nuclear Engineering Division

About Argonne National Laboratory
Argonne is a U.S. Department of Energy laboratory managed by UChicago Argonne, LLC under contract DE-AC02-06CH11357. The Laboratory's main facility is outside Chicago, at 9700 South Cass Avenue, Argonne, Illinois 60439. For information about Argonne and its pioneering science and technology programs, see www.anl.gov.

DOCUMENT AVAILABILITY

Online Access: U.S. Department of Energy (DOE) reports produced after 1991 and a growing number of pre-1991 documents are available free via DOE's SciTech Connect (http://www.osti.gov/scitech/)

Reports not in digital format may be purchased by the public from the National Technical Information Service (NTIS):
U.S. Department of Commerce
National Technical Information Service
5301 Shawnee Rd
Alexandra, VA 22312
www.ntis.gov
Phone: (800) 553-NTIS (6847) or (703) 605-6000
Fax: (703) 605-6900
Email: **orders@ntis.gov**

Reports not in digital format are available to DOE and DOE contractors from the Office of Scientific and Technical Information (OSTI):
U.S. Department of Energy
Office of Scientific and Technical Information
P.O. Box 62
Oak Ridge, TN 37831-0062
www.osti.gov
Phone: (865) 576-8401
Fax: (865) 576-5728

Disclaimer
This report was prepared as an account of work sponsored by an agency of the United States Government. Neither the United States Government nor any agency thereof, nor UChicago Argonne, LLC, nor any of their employees or officers, makes any warranty, express or implied, or assumes any legal liability or responsibility for the accuracy, completeness, or usefulness of any information, apparatus, product, or process disclosed, or represents that its use would not infringe privately owned rights. Reference herein to any specific commercial product, process, or service by trade name, trademark, manufacturer, or otherwise, does not necessarily constitute or imply its endorsement, recommendation, or favoring by the United States Government or any agency thereof. The views and opinions of document authors expressed herein do not necessarily state or reflect those of the United States Government or any agency thereof, Argonne National Laboratory, or UChicago Argonne, LLC.

ANL/NE-16/29

Initial Comparison of Direct and Legacy Neutronics Modeling Approaches for Radial Core Expansion Analysis

prepared by
Emily R. Shemon
Nuclear Engineering Division, Argonne National Laboratory

October 10, 2016

ABSTRACT

Radial core expansion in sodium-cooled fast reactors provides an important reactivity feedback effect. As the reactor power increases due to normal start up conditions or accident scenarios, the core and surrounding materials heat up, causing both grid plate expansion and bowing of the assembly ducts. When the core restraint system is designed correctly, the resulting structural deformations introduce negative reactivity which decreases the reactor power. Historically, an indirect procedure has been used to estimate the reactivity feedback due to structural deformation which relies upon perturbation theory and coupling legacy physics codes with limited geometry capabilities.

With advancements in modeling and simulation, radial core expansion phenomena can now be modeled directly, providing an assessment of the accuracy of the reactivity feedback coefficients generated by indirect legacy methods. Recently a new capability was added to the PROTEUS-SN unstructured geometry neutron transport solver to analyze deformed meshes quickly and directly. By supplying the deformed mesh in addition to the base configuration input files, PROTEUS-SN automatically processes material adjustments including calculation of region densities to conserve mass, calculation of isotopic densities according to material models (for example, sodium density as a function of temperature), and subsequent re-homogenization of materials.

To verify the new capability of directly simulating deformed meshes, PROTEUS-SN was used to compute reactivity feedback for a series of contrived yet representative deformed configurations for the Advanced Burner Test Reactor design. The indirect legacy procedure was also performed to generate reactivity feedback coefficients for the same deformed configurations. Interestingly, the legacy procedure consistently overestimated reactivity feedbacks by 35% compared to direct simulations by PROTEUS-SN. This overestimation indicates that the legacy procedures are in fact not conservative and could be overestimating reactivity feedback effects that are closely tied to reactor safety. We conclude that there is indeed value in performing direct simulation of deformed meshes despite the increased computational expense. PROTEUS-SN is already part of the SHARP multi-physics toolkit where both thermal hydraulics and structural mechanical feedback modeling can be applied but this is the first comparison of direct simulation to legacy techniques for radial core expansion.

Table of Contents

Abstract i
Table of Contents iii
List of Figures iv
List of Tables iv
1 Introduction 1
2 Direct Modeling with PROTEUS-SN 2
2.1 Coupled Calculations with SHARP Toolkit 2
2.2 New Capability for Standalone Calculations 2
3 Modeling with Conventional Tools 3
3.1 Coupled Calculations with Conventional Tools 3
3.2 Modified Procedure for Standalone Neutronics 3
4 Calculation of Radial Core Expansion Reactivity Feedback in the ABTR Design 4
4.1 Undeformed Configuration 5
4.2 Calculation of Reactivity Feedback with DIF3D/PERSENT 7
5 Conclusions 13
6 References 14

LIST OF FIGURES

Figure 1. Deformation States for a Limited Free Bow Restraint System showing a) Undeformed (Base State), (b) Intermediate Deformation State, (c) Limited Free Bow (end state). 1
Figure 2. Consistent Workflow to Compare Perturbation-based and Directly Calculated Reactivity Feedback from Radial Core Expansion: (a) Undeformed Mesh Simulation and (b) Deformed Mesh Simulation. 4
Figure 3. Core Map of the Advanced Burner Test Reactor. 5
Figure 4. PROTEUS-SN Computed Multigroup Fluxes at Plane Z=150 for Base Configuration. Upper Row: Group 1 (6.06-14.19 MeV), Group 10 (67.4-111.1 keV), Bottom Row: Group 17 (2.03-3.35 keV), Group 19 (0.454-1.23 keV). 6
Figure 5. PROTEUS-SN Normalized Power Distribution at Z=150 (left) and Y=0 (right) for Base Configuration. 6
Figure 6. Region-Dependent Reactivity Worth Calculated by PERSENT (P5) for 1% Increase in Fuel Density. (left) Slice taken at Y=0, (right) Slice taken at Z=150 cm (active core zone). 8
Figure 7. Region Dependent Reactivity Worth Calculated by PERSENT (P5) for 1% Increase in Structure Density (left) or Sodium Density (right). Both slices taken at Y=0. 9
Figure 8. Radial Core Deformation Schemes Applied for ABTR Analysis. 11

LIST OF TABLES

Table 1. Eigenvalues Computed for the Base (Undeformed) State of the ABTR. 5
Table 2. Whole Core Reactivity Coefficients for the ABTR Calculated by DIF3D-VARIANT/PERSENT per 1% Increase in Fuel, Structure, and Sodium Density. 8
Table 3. Radial Core Deformation Schemes Applied for ABTR Analysis. 11
Table 4. Computed Reactivity Worths for ABTR Deformation Schemes. 12

1 Introduction

Radial core expansion in sodium-cooled fast reactors provides an important reactivity feedback effect. As the reactor power increases due to normal start up conditions or accident scenarios, the core and surrounding materials heat up causing both grid plate expansion and bowing of the assembly ducts. The core restraint system can be designed to guide the assembly movement into a free bow or limited free bow shape, both of which introduce negative reactivity feedback to the core. As time proceeds, the assembly deformation changes include both compaction and expansion at different regions, but once the assemblies contact each other at the above core load pad (ACLP) elevation which is part of the restraint system, the reactor is "locked up" and unable to compact any further [1], shown in Figure 1(c). Typically the core is designed such that this locked up state provides negative reactivity from the base configuration, and any further heating will cause outward bowing of the fuel assemblies and hence further negative reactivity feedback. Therefore, as the power and temperature increases, there exists a natural upper limit to these quantities as negative reactivity will be inserted once thermal expansion reaches the locked up state.

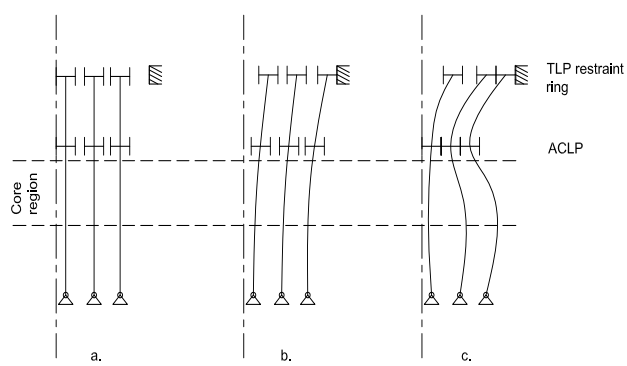

Figure 1. Deformation States for a Limited Free Bow Restraint System showing a) Undeformed (Base State), (b) Intermediate Deformation State, (c) Limited Free Bow (end state).

With advancements in modeling and simulation, radial core expansion phenomena can be modeled directly, providing an assessment of the accuracy of the reactivity feedback coefficients generated by indirect methods which are used in design today (in some cases, these coefficients are not used at all due to lack of confidence in their accuracy). Recently a new capability was added to the PROTEUS-SN unstructured geometry neutron transport solver to analyze deformed meshes quickly and directly. By supplying the deformed mesh in addition to the base configuration input files, PROTEUS-SN automatically processes material adjustments including calculation of region densities to conserve mass, calculation of isotopic densities according to material models (for example, sodium density as a function of temperature), and subsequent re-homogenization of materials.

In this report the new PROTEUS-SN direct modeling capability is initially assessed by comparing reactivity worths for radial core deformation schemes against the same values calculated using legacy approaches.

2 Direct Modeling with PROTEUS-SN

The PROTEUS-SN code [2,3,4] developed at Argonne National Laboratory solves neutron transport problems defined on an unstructured finite element mesh. The unstructured finite element capability differentiates PROTEUS-SN from most other transport solvers which are limited to a semi-structured grid at best (repeated lattice with detailed pins), with extruded geometry in the axial direction. The modeling of deformed geometry is mathematically identical to the modeling of undeformed geometry in PROTEUS-SN by nature of the finite element method. This is by design as one of PROTEUS-SN's original intended applications was the modeling of structural reactivity feedback effects in sodium-cooled fast reactors.

2.1 Coupled Calculations with SHARP Toolkit

Inside the NEAMS-developed SHARP Toolkit [5], PROTEUS-SN is coupled to the Diablo [6] structural mechanics code and the Nek5000 [7] thermal hydraulics code. PROTEUS-SN provides power distribution data to Nek5000, Nek5000 computes temperature distributions, and upon power and temperature convergence Diablo computes the resulting structural deformation. Previous analysis [8] was performed to compute the reactivity feedback resulting from thermal expansion of the Advanced Burner Test Reactor design [9] with a preliminary restraint ring design [10]. This year, capabilities were added to PROTEUS-SN to automate the processing of material properties for deformed meshes in SHARP calculations. For example, sodium should backfill part of the expanded geometry, and such regions must be re-homogenized according to new material concentrations. The density of regions are otherwise be adjusted to preserve mass.

Due to the considerable complexity in setting up detailed models for the three physics within SHARP analysis, a new capability was recently added to PROTEUS-SN to facilitate standalone simulations of deformed meshes.

2.2 New Capability for Standalone Calculations

A new capability was added to PROTEUS-SN to analyze deformed meshes quickly and directly outside of the SHARP framework by supplying the deformed mesh in addition to the base configuration input files. PROTEUS-SN automatically processes all material adjustments including re-calculation of region densities to conserve mass, re-calculation of isotopic densities according to material models (for example, sodium density as a function of temperature), and subsequent re-homogenization of materials as necessary.

To test the new capability, a separate utility has been created under the PROTEUS Mesh Tools collection [11] to quickly generate deformed 3D finite element meshes according to user-specified strain functions. For simplicity, the strain functions can only vary with the Z-coordinate as there is no way to distinguish geometrical features such as assemblies in the X-Y plane with the currently stored finite element data. While in reality assemblies should be permitted to deform according to unique axial shapes (outer vs. inner, fuel vs. reflector, etc), this tool provides an approximate deformation scheme for testing purposes. A more advanced mesh deformation tool can be created in the future.

3 Modeling with Conventional Tools

3.1 Coupled Calculations with Conventional Tools

The geometry limitations of conventional codes prevent the direct modeling of radial core expansion reactivity feedback effects, which result in complex geometry changes that cannot be modeled on a structured grid. Instead, an indirect procedure [12] is used to estimate the reactivity feedback due to structural deformation:

1. Perform a DIF3D [13,14] neutronics calculation of the undeformed (base) state to compute the eigenvalue, forward flux, and adjoint flux.

2. Separately perturb the number densities of fuel, sodium, and structural isotopes in selected regions and use the perturbation and sensitivity analysis code VARI3D [15] to calculate the reactivity coefficient due to these perturbations ($\frac{\partial \rho}{\partial D_{m,i}}$, where $\partial D_{m,i}$ is the change in density of material m in region i). The density perturbation is assumed to be a direct consequence of homogenizing materials over new volumes due to core expansion/contraction.

3. Use SuperEnergy-2 [16] (temperature data) and NUBOW-3D [1] (mechanical deformation code restricted to 1/12 core symmetry) to calculate the region-wise deformation and density changes due to thermal expansion. NUBOW-3D processes the VARI3D mesh-based reactivity coefficients to obtain the total core expansion reactivity coefficient for the particular deformation scenario.

The conventional procedure assumes the density perturbations are small (valid regime of perturbation theory), the effect of the geometrical expansion coupled with the density perturbations can be neglected, the density perturbations of different isotope types (fuel, sodium, structure) are decoupled, the coupling effect of space-variation of density perturbations in different areas is ignored, and 1/12 core symmetry restriction is imposed by NUBOW-3D.

3.2 Modified Procedure for Standalone Neutronics

Here we focus on consistent neutronics modeling of a particular deformed geometry case, so the conventional procedure was simplified by substituting known deformation shapes in place of using SE-2 and NUBOW-3D. These deformation shapes induce local density changes which are then processed with PERSENT [17,18] (modern replacement for VARI3D) mesh-based reactivity feedback coefficients to compute the total reactivity feedback, as shown in Figure 2. The PERSENT reactivity feedback coefficients are calculated using the base configuration DIF3D-VARIANT transport code [19] flux files along with arbitrary material density perturbations.

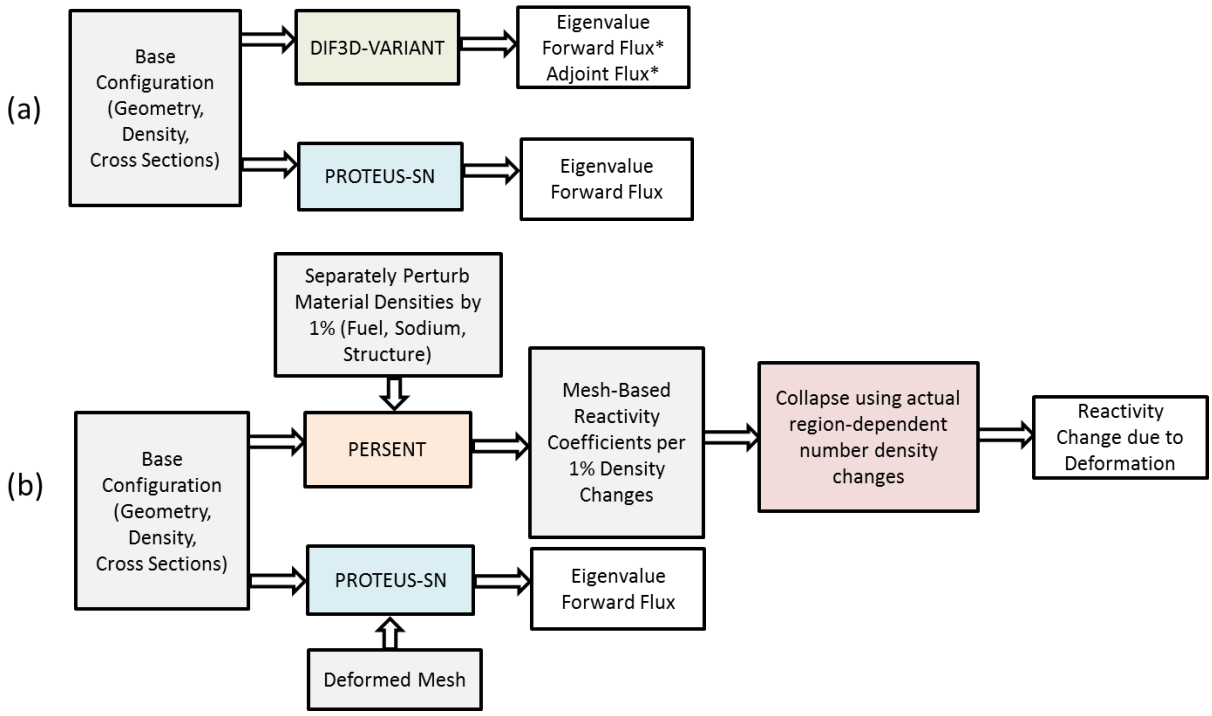

Figure 2. Consistent Workflow to Compare Perturbation-based and Directly Calculated Reactivity Feedback from Radial Core Expansion: (a) Undeformed Mesh Simulation and (b) Deformed Mesh Simulation.

The assumed deformation shape is modeled directly using PROTEUS-SN by processing the base configuration mesh with the mesh deformation utility tool described previously. The two neutronics models (DIF3D and PROTEUS-SN) are entirely consistent (same geometry, cross section data, and homogenized assembly regions).

4 Calculation of Radial Core Expansion Reactivity Feedback in the ABTR Design

The Advanced Burner Test Reactor (ABTR) core design [9,10] was chosen as a test case because DIF3D models were readily available. The material compositions and axial dimensions differ slightly from previous PROTEUS-SN models of the ABTR. The ABTR core, shown in Figure 3, consists of 199 assemblies arranged in a hexagonal grid with 9 rings. The core contains three different fuel assembly types as well as control, shield, and reflector assemblies. The assemblies labeled “Material Test” were replaced with reflector assemblies in the model. Axially, the core extends from 0.0 cm to 345.68 cm elevation where the active core is located between 110.54 cm and 194.95 cm elevation. The assembly pitch is 14.685 cm.

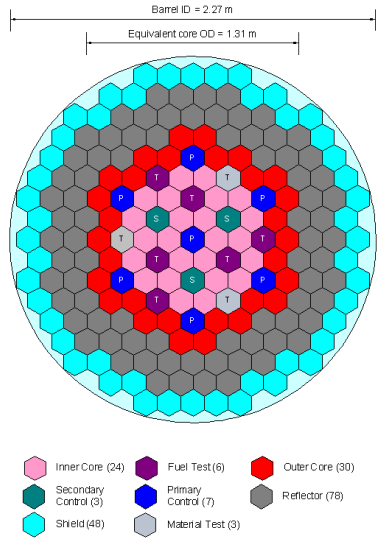

Figure 3. Core Map of the Advanced Burner Test Reactor.

4.1 Undeformed Configuration

The base configuration (undeformed geometry) with homogenized assemblies was simulated with PROTEUS-SN and DIF3D-VARIANT using a common 21 energy group cross section data file. Results are summarized in Table 1. Multigroup flux distributions and power distributions calculated in PROTEUS-SN are shown in Figure 4 and Figure 5. Note that power distributions are discontinuous across assembly boundaries due to material changes. A PN convergence study was partially performed for DIF3D-VARIANT which showed increasing eigenvalue as the PN order was increased, as expected. Recent work [20] showed that L7T7 cubature (SN method) is sufficiently converged for PROTEUS-SN for the ABTR homogeneous geometry configuration. Spatial convergence studies were not performed for either code due to time limitations, but reasonable accuracy is expected using the parameters shown. We note that 100-200 pcm discrepancies are expected between DIF3D and PROTEUS-SN solutions due to inconsistent χ fission neutron distribution treatment in the two codes. Note that PROTEUS-SN provides more accurate solutions in terms of the fission spectrum. The two codes are in agreement within this tolerance for the base configuration.

Table 1. Eigenvalues Computed for the Base (Undeformed) State of the ABTR.

Code and Options	**Base (Undeformed) Eigenvalue**
DIF3D-VARIANT 040601 space, 41 axial regions (8-10 cm mesh), P1 scattering, 21 energy groups	1.02087 (P3) 1.02226 (P5) 1.02273 (P7)
PROTEUS-SN Quadratic FEM (6 triangles/ assembly, 41 axial regions), L7T7 cubature (128 angles on sphere), P1 scattering, 21 energy groups	1.02119

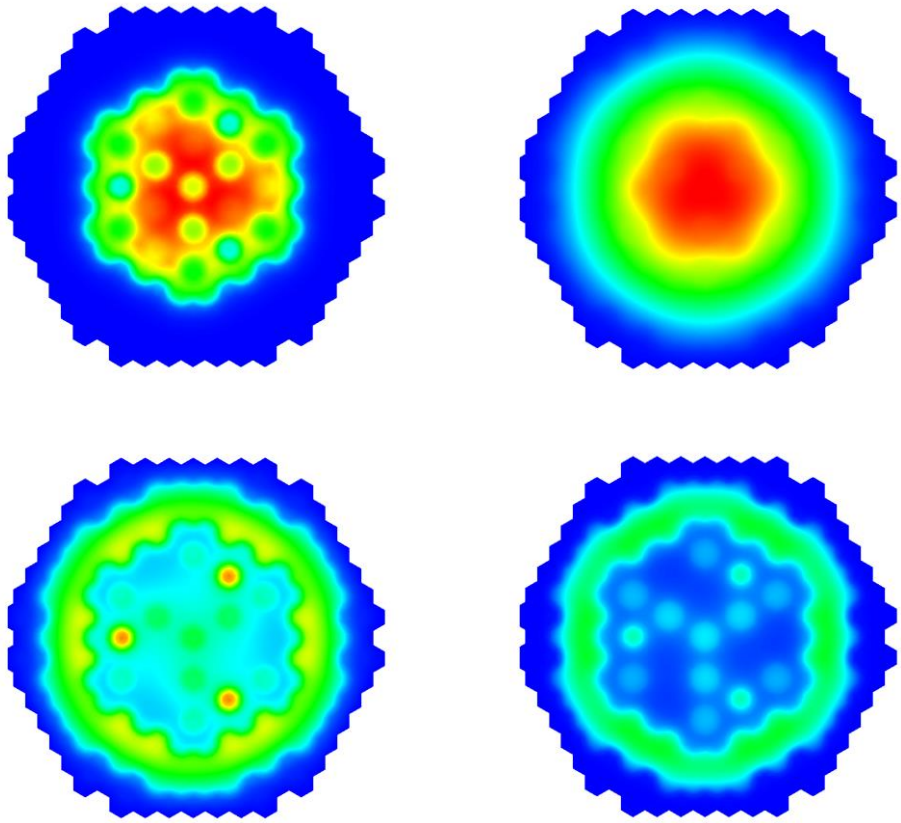

Figure 4. PROTEUS-SN Computed Multigroup Fluxes at Plane Z=150 for Base Configuration. Upper Row: Group 1 (6.06-14.19 MeV), Group 10 (67.4-111.1 keV), Bottom Row: Group 17 (2.03-3.35 keV), Group 19 (0.454-1.23 keV).

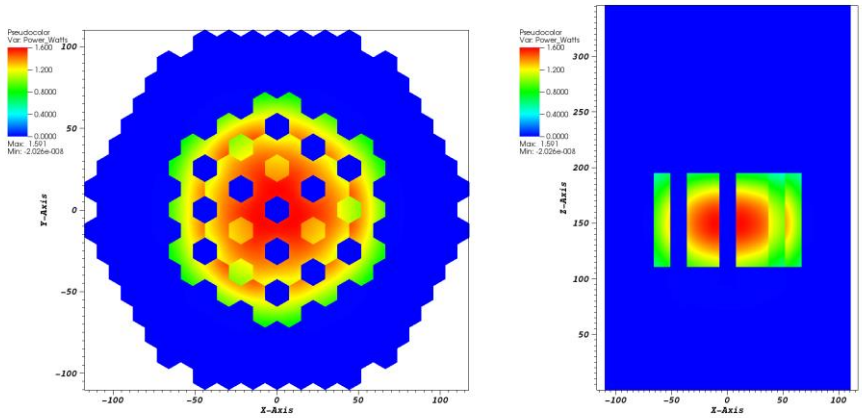

Figure 5. PROTEUS-SN Normalized Power Distribution at Z=150 (left) and Y=0 (right) for Base Configuration.

4.2 Calculation of Reactivity Feedback with DIF3D/PERSENT

As illustrated in Figure 2(b), the DIF3D/PERSENT procedure to compute reactivity feedback from radial core expansion is a two-step procedure. In the first step, generalized 1% fuel, structure, and sodium density perturbations are applied to the base configuration to estimate region-dependent reactivity changes, $\frac{\partial \rho}{\partial D_{m,i}}$, where m is {fuel, structure, sodium} and i is the mesh region. This calculation is not dependent on a specific deformation. These region-wise quantities are then post-processed in a second step using the region-wise material density changes in the deformed state, $\Delta D_{m,i}$, to yield the total reactivity change:

$$\Delta\rho = \sum_{m=fuel,sod,struct} \sum_{i=1}^{N} \left(\frac{\partial \rho}{\partial D_{m,i}} \right) \Delta D_{m,i} \tag{1}$$

The whole core reactivity feedback coefficients, i.e., the reactivity introduced for a 1% change in density of material {fuel, sodium, and structure} over the entire system are calculated by PERSENT for the ABTR core and reported in Table 2. however, these quantities are not directly used in these calculations. These coefficients were computed for both P3 and P5 angular order in VARIANT, and observed to be nearly independent of PN order. Note that the sodium density reactivity coefficient fluctuated from negative to positive upon increasing the PN order, but the value is so small compared to the fuel and structure coefficients, it can be neglected. Additionally, in this radial core expansion study, constant sodium density was maintained so this factor is not even used.

The region-wise reactivity coefficients were calculated on a mesh consisting of 41 8-10 cm axial segments (11 segments within the active core zone) and 9 radial rings. Similar assemblies within the same ring were grouped together to take advantage of radial symmetry. Since the perturbations applied in this work are all symmetric about the core center, all assemblies within a given ring undergo the same density changes and therefore this grouping does not matter. Slices along the Y=0 plane were taken of the region-wise reactivity coefficients computed by PERSENT and plotted in Figure 6 (fuel perturbation) and Figure 7 (structure and sodium perturbations).

Figure 6 shows that the fuel assemblies closest to the core center have the highest reactivity worth, as expected. Additionally, the axial middle of the core has the highest reactivity worth. The reactivity worth of a fuel assembly is at most 15 pcm (1.5E-6 on the chart) per 1% change in fuel density, per axial zone (8-10 cm segment). The fuel assemblies have strictly positive reactivity worths because an increase in fuel density anywhere in the core implies core compaction or an increase in fissionable material and production of neutrons.

Table 2. Whole Core Reactivity Coefficients for the ABTR Calculated by DIF3D-VARIANT/PERSENT per 1% Increase in Fuel, Structure, and Sodium Density.

	PERSENT + DIF3D-VARIANT P3	PERSENT + DIF3D-VARIANT P5
$\frac{\partial \rho}{\partial D_{fuel}}$	4.53901E-03 (+454 pcm)	4.52323E-03 (+452 pcm)
$\frac{\partial \rho}{\partial D_{structure}}$	2.09060E-04 (+21 pcm)	2.02391E-04 (+20 pcm)
$\frac{\partial \rho}{\partial D_{sodium}}$	6.91301E-06 (+0.7 pcm)	-3.66336E-06 (-0.4 pcm)

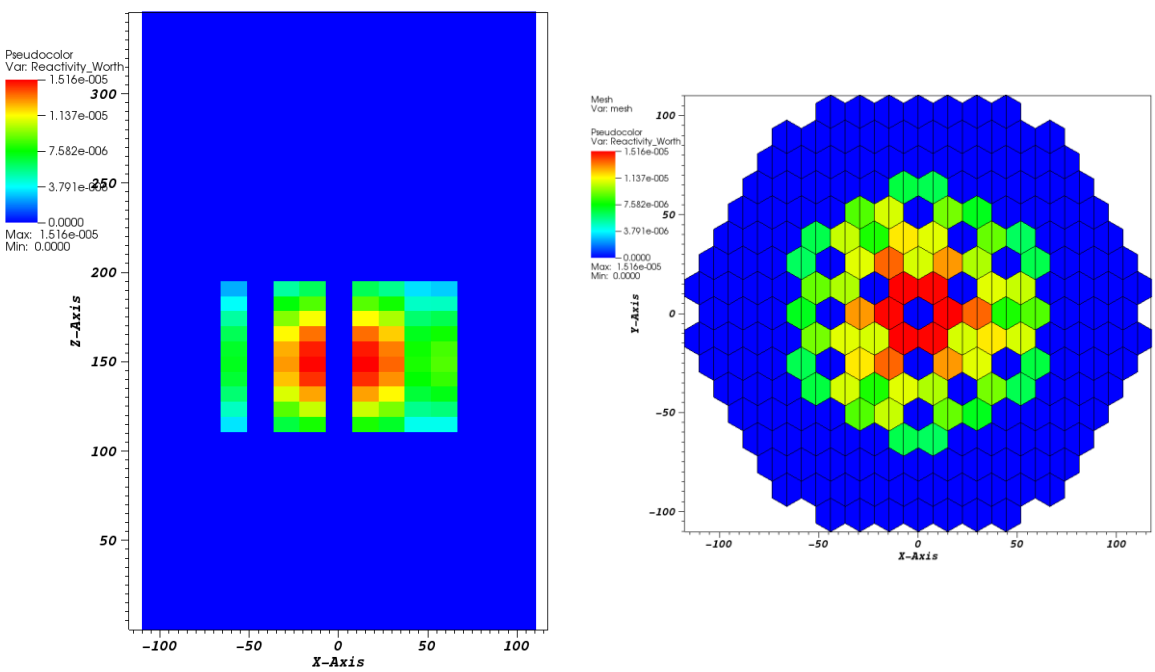

Figure 6. Region-Dependent Reactivity Worth Calculated by PERSENT (P5) for 1% Increase in Fuel Density. (left) Slice taken at Y=0, (right) Slice taken at Z=150 cm (active core zone).

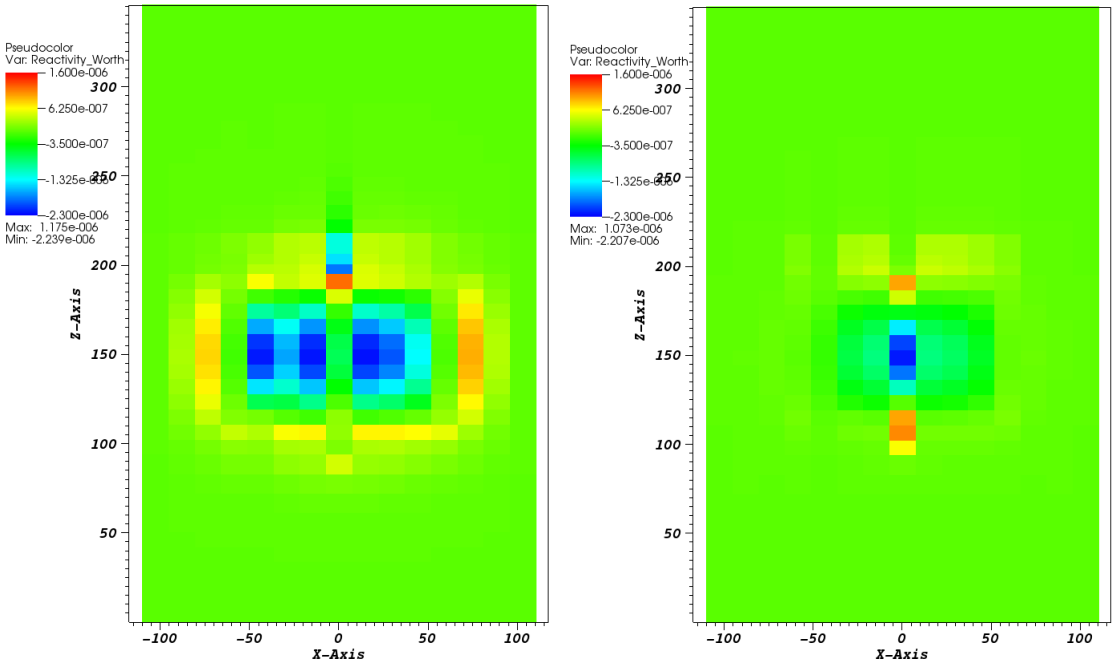

Figure 7. Region Dependent Reactivity Worth Calculated by PERSENT (P5) for 1% Increase in Structure Density (left) or Sodium Density (right). Both slices taken at Y=0.

Figure 7 shows the reactivity worth for 1% perturbation in structural density (left) or sodium density (right). The legend extents on these two plots have the same color scale for direct comparison. One can immediately note that the maximum region-wise reactivity worth of both structural and sodium density changes are roughly 5-10x smaller in magnitude than those due to fuel density changes. Thus the reactivity feedback will be dominated by fuel density changes. Also notable is that sodium density reactivity worth is negligible (<<1 pcm) in nearly all regions except the central control rod where it is negative (-2.3 pcm) in the center of the active core and positive at the bottom and top of the active core. Overall the mesh-dependent sodium reactivity worths appear to roughly cancel each other out provided a uniform core-wide perturbation is applied. This is consistent with the very small (~-0.4 to 0.7 pcm) values reported in Table 2. Looking at these values, we should expect the perturbations performed at the axial center of the active core to have the largest impact on reactivity. Perturbations well above and below the active core should not result in large reactivity changes.

A variety of deformation cases were strategically chosen to compare accuracy of the legacy technique to a direct modeling approach (PROTEUS-SN). The deformations are applied such that the pitch of all assemblies in an X-Y plane (same Z-elevation) changes identically. The change in assembly pitch is plotted as a function of Z for the different cases in Figure 8 and tabulated in Table 3. Data points are linearly interpolated between specified Z-elevations.

Case I is a free flowering shape based on the assumption that fuel assemblies should bow no more 0.2 mm from centerline. Grid plate expansion is ignored, and the deformations are assumed to represent bowing. The general shape chosen is similar to that in Figure 1(b) with representative numbers chosen after discussion with an expert in nuclear reactor structural mechanics for a different reactor design [21].

Case II is representative of an intermediate state in a limited free bow design (not locked up yet), whereby the expansion in the active core initially bows inward, producing positive reactivity. More information on this is given in [1].

Case III applies a uniform radial grid expansion of 0.596% (which yields a change in assembly pitch of +0.88 mm based on a 146.85 mm base pitch). This radial expansion factor at operating condition was taken from the ABTR Specification Report [10].

Case IV and Case IV incorporate the uniform radial grid expansion from Case III as well as the deformation shapes from Case I and Case II, respectively.

We emphasize that the deformation shapes modeled applied here are contrived and at best considered to be somewhat “representative” - they are not implied to be the true deformation that would occur. To obtain the true deformation, direct coupling with structural mechanics code and complete description of the core restraint system would be required via the SHARP Toolkit (in fact, this was previously done in past years under NEAMS but without the automatic density adjustment capabilities new to this year’s work). The purpose of this work is to compare conventional techniques to the new direct modeling approach using consistent models and deformations for fair comparison. Additionally, contrary to real deformation shapes, typically the outer reflector and shield assemblies do not bow and deform as much as indicated here.

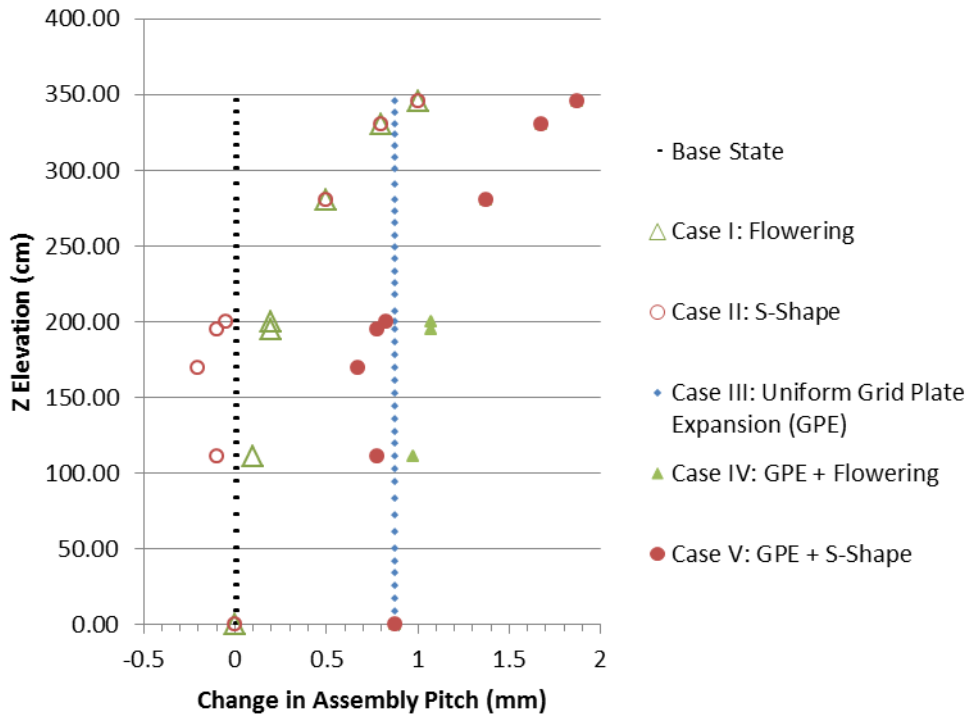

Figure 8. Radial Core Deformation Schemes Applied for ABTR Analysis.

Table 3. Radial Core Deformation Schemes Applied for ABTR Analysis.

		Change in Assembly Pitch (mm) Base Case Assembly Pitch=146.85 mm				
Geometry	**Elevation (cm)**	**Case I**	**Case II**	**Case III**	**Case IV**	**Case V**
Above Active Core	345.68	1.0	1.0	0.88	1.88	1.88
	330.61	0.8	0.8	*	1.68	1.68
	280.36	0.5	0.5	*	1.38	1.38
ACLP Elevation	200.0	0.2	-0.05	*	1.08	0.83
Active Core	194.95	0.2	-0.1	*	1.08	0.77
	169.63	*	-0.2	*	*	0.67
	110.54	0.1	-0.1	*	0.98	0.78
Bottom	0.0	0.0	0.0	0.88	0.88	0.88

PROTEUS-SN directly computes the volume change in each mesh region (with regions identically defined in DIF3D), so the volume changes due to deformation are easily translated to isotopic density changes and processed against the PERSENT region-based reactivity coefficients. Direct simulations of the deformed mesh were performed using PROTEUS-SN. The eigenvalue and reactivity worth results are summarized in Table 4. As expected, all of the reactivity worths are negative expect for Case II, since Case II is the only deformation scheme that pushes fuel material closer to the core centerline than the based configuration. While flux and power solutions were easily generated for the deformed cases, it is not worthwhile to compare them visually against the undeformed base case, since differences are too small to discern and the powers are normalized inside the code before printing.

The PROTEUS-SN-computed reactivity worths for Case I (-70) and Case II (+69) are nearly identical, just opposite in sign, even though the deformation shapes are significantly different. However the deformation shapes within the active core are similar (but in opposite directions). The region-wise distribution of reactivity worths computed by PERSENT predicted that only changes near the active core would contribute non-negligibly to reactivity worth, and this is confirmed in the comparison between Case I and Case II.

The PROTEUS-SN-computed reactivity worth of Case III, uniform grid plate expansion (-413 pcm) is much higher in magnitude than the initial Case I and Case II assembly bowing deformation schemes (-70 and +69 pcm respectively). Therefore the grid plate expansion is a significant effect that must be considered. Case IV is simply a superposition of the Case I and Case III deformation shapes and interestingly, the reactivity worth of this case is also the superposition of the reactivity worths of those two calculations. A similar statement holds for Case V. This suggests that these perturbations cause highly linear changes in reactivity, and the reactivity coefficients predicted by PERSENT/DIF3D-VARIANT are actually quite accurate for a large regime of values.

Table 4. Computed Reactivity Worths for ABTR Deformation Schemes.

		Predicted Reactivity Worth of Deformation				
Code	**Value**	**Case I**	**Case II**	**Case III**	**Case IV**	**Case V**
PERSENT/DIF3D-VARIANT (P5)	$\Delta\rho$ (pcm)	-95	+98	-558	-652	-463
PROTEUS-SN	k	1.02046	1.02191	1.01690	1.01618	1.01762
	$\Delta\rho$ (pcm)	-70	+69	-413	-483	-343
% Difference in Reactivity Worth	$\frac{PERSENT - PROTEUS}{PROTEUS}$	+35%	+42%	+35%	+35%	+35%

However, in all cases, the DIF3D-based PERSENT calculations overestimate the reactivity worth of a given deformation scheme by approximately 35% compared to PROTEUS-

SN (direct computation). This overestimation is important to note, because it means that the legacy calculation is not conservative. In reactor safety analysis, safety margins must be used to protect against uncertainty or error in calculations. While the legacy procedure produces answers that are comparable to PROTEUS-SN results and follow the same trends, the bias in the answer raises uncertainty in using this technique for arbitrary calculations. This bias is likely arising from the fact that geometry changes are not accounted for in the perturbation theory method, and therefore a 1% increase in fuel density perturbation is actually adding fuel to the system, when in reality the mass of fuel should be conserved. Additionally, the legacy procedure does not take into account combined effects, i.e. in these deformation schemes, the structure and fuel densities change together. The lack of modeling of the physics interplay between these two materials could be contributing to some of the error.

In conclusion, the legacy method produced reactivity worth values for radial core expansion of the ABTR which follow the expected trends, but are non-conservative by at least 35%. Utilizing the legacy-computed values for reactor design could result in overprediction of negative reactivity feedback for a radial core expansion scenario, possibly resulting in an unsafe operating regime.

We also note that the PROTEUS-SN calculations were consistently performed for homogeneous assembly geometry in this case. There is likely a bias effect due to non-explicit modeling of the assembly ducts and fuel pins. This should be explored in the future. Additionally, such heterogeneous modeling will be essential to deforming the mesh according to more complex functions of space.

In the future, we plan to add a capability to deform meshes based on NUBOW-3D data. That case requires more complex movement of assemblies and identification of assembly features which is not currently necessary or implemented in PROTEUS-SN since it is based on the general finite element method.

5 Conclusions

A new capability was added to the PROTEUS-SN code to quickly analyze deformed mesh configurations. In particular, the code can be used in standalone mode to analyze a deformed mesh. All material densities are updated automatically by the code at runtime based on geometrical changes from the undeformed configuration and material models specified by the user. When used in coupled mode via SHARP, the material densities are also updated automatically which significantly streamlines analysis of radial core expansion problems. The current material model included is for computing liquid sodium density as a function of temperature. Homogenization and adjustment of homogenized densities is calculated automatically if sodium backfill is selected due to mesh deformation.

PROTEUS-SN's new mesh deformation capability was verified against legacy procedures to compute reactivity worth of deformation schemes for the ABTR design using a series of contrived but somewhat realistic deformation schemes. The PROTEUS-SN computed reactivity worths were more conservative (smaller in magnitude) then the conventionally computed quantities. More work is needed to see if the conservatism applies across all reactor cores.

In order to expand PROTEUS-SN's mesh deformation modeling demonstration, a utility should be created to apply realistic geometry perturbations to reactor geometries, in particular the ability to perform grid plate expansion separate from bowing. This would allow, for example, the ducts to bow expanding their thickness (maintaining the same volume, but increasing/decreasing the distance between duct walls). Such a utility can be written based on the UFmesh format by adding some logic and storage for defining geometry features (solid, liquid, fuel pin, duct, etc). The UFmesh format is particularly suitable for modification by NUBOW type data which propagates assembly pitch, and assembly location translation. The ideal work would be to update NUBOW-3D to full core geometry (currently limited to 1/12 core symmetry) and directly calculated structural mechanical changes using power distributions computed by PROTEUS-SN and temperatures from some external code. We note that the transport solver of PROTEUS-SN is fully ready today to perform such a calculation for any type of deformed mesh - the creation of the mesh itself is the bottleneck.

6 References

1. J. J. Grudzinski and C. Grandy, "Design and Analysis of the Core Restraint System for a Small Modular Fast Reactor", *Transactions of the 22nd Conference on Structural Mechanics in Reactor Technology (SMiRT-22)*, San Francisco, CA, USA, August 18-23, 2013.
2. E. R. Shemon, C. H. Lee, M. A. Smith, and A. Marin-Lafleche, "NEAMS Neutronics: Development and Validation Status," Proceedings of ICAPP 2014, Charlotte, USA, April 6-9, 2014 [CD-ROM].
3. E. R. Shemon, M. A. Smith, and C. H. Lee, "PROTEUS-SN Methodology Manual," ANL/NE-14/5, Argonne National Laboratory, June 30, 2014.
4. E. R. Shemon, M. A. Smith, C. H. Lee, and A. Marin-Lafleche "PROTEUS-SN User Manual," ANL/NE-14/6, Argonne National Laboratory, June 30, 2014.
5. Y. Yu, E. R. Shemon, J. W. Thomas, V. Mahadevan, R. Rahaman, J. Solberg, "SHARP User Manual", Argonne National Laboratory Report ANL-NE-16/6, March 31, 2016.
6. D. Parsons, J. M. Solberg, R. M Ferencz, M. A. Havstad, N. E. Hodge, A. P Wemhoff, "Diablo User Manual", Lawrence Livermore National Laboratory Report UCRL-SM-234927, September 2007.
7. P. F. Fischer, J. W. Lottes, S. G. Kerkemier, Nek5000 Web Page, http://nek5000.mcs.anl.gov, 2008.
8. E. Merzari, E. Shemon, Y. Yu, J. Thomas, A. Obabko, R. Jain, V. Mahadevan, J. Solberg, R. Ferencz, R. Whitesides, "Full Core Multi-Physics Simulation with Offline Core Deformation", Argonne National Laboratory Report ANL-NE-15/42, December 21, 2015.
9. Y. I. Chang, et al, "Advanced Burner Test Reactor Preconceptual Design Report", ANL-ABR-1 (ANL-ACFI-173), Argonne National Laboratory, September 5, 2006.
10. E. R. Shemon, J. J. Grudzinski, C. H. Lee, J. W. Thomas, and Y. Q. Yu, "Specification of the Advanced Burner Test Reactor Multi-Physics Coupling Demonstration Problem", ANL/NE-15/43, Argonne National Laboratory, December 21, 2015.

11. M. A. Smith and E. R. Shemon, "User Manual for the PROTEUS Mesh Tools," ANL/NE-15/17 Rev.1, Argonne National Laboratory, June 1, 2015.
12. T. K. Kim, Personal Communication, Argonne National Laboratory, August 2016.
13. K. L. Derstine, "DIF3D: A Code to Solve One-, Two-, and Three-Dimensional Finite-Difference Diffusion Theory Problems," ANL-82-64, Argonne National Laboratory (1984).
14. R. D. Lawrence, "The DIF3D Nodal Neutronics Option for Two- and Three-Dimensional Diffusion Theory Calculations in Hexagonal Geometry," ANL-83-1, Argonne National Laboratory, March 1983.
15. C. H. Adams, "Specifications for VARI3D—A Multidimensional Reactor Design Sensitivity Code," FRA-TM-74, Argonne National Laboratory (1975).
16. K. L. Basehorea and N. E. Todreas, "SUPERENERGY-2: A Multiassembly, Steady-State Computer Code for LMFBR Core Thermal-Hydraulic Analysis", PNL-3379 (COO-2245-57TR, UC-72), Pacific Northwest Laboratory, Richland, Washington, August 1980.
17. M. A. Smith, et al., "VARI3D & PERSENT: Perturbation and Sensitivity Analysis," ANL/NE-13/8 (2013).
18. M. A. Smith, W. S. Yang, A. Mohamed, E. E. Lewis, "Perturbation and Sensitivity Tool Based on the VARIANT Option of DIF3D," American Nuclear Society Transactions 107, San Diego, CA, Nov. 11-15 (2012).
19. G. Palmiotti,E. E. Lewis, C. B. Carrico, "VARIANT: VARIational Anisotropic Nodal Transport for Multidimensional Cartesian and Hexagonal Geometry Calculation," Argonne National Laboratory ANL-95/40, 1995.
20. M. G. Jarrett, E. R. Shemon, C. H. Lee, M. A. Smith, "Heterogeneous Multigroup Cross Sections for Fast Reactor Calculations with MC2-3/PROTEUS", Proceedings of PHYSOR 2016, Sun Valley, Idaho.
21. J. J. Grudzinski, Personal Communication, Argonne National Laboratory, August and September 2016.

Nuclear Engineering Division
Argonne National Laboratory
9700 South Cass Avenue, Bldg. 208
Argonne, IL 60439

www.anl.gov

Argonne National Laboratory is a U.S. Department of Energy
laboratory managed by UChicago Argonne, LLC